10 MW, 0.14 THz, CW Gyrotron and Optical Transmission System for Millimeter Wave Heating of Plasmas in the Stellarator W7-X

M.Thumm*, G. Dammertz, G. Gantenbein, S. Illy, S. Kern, W. Leonhardt, G. Neffe, B. Piosczyk, M. Schmid
Forschungszentrum Karlsruhe, Association Euratom-FZK,
Institut für Hochleistungsimpuls- und Mikrowellentechnik,
Postfach 3640, 76021 Karlsruhe, Germany
*Universität Karlsruhe, Institut für Höchstfrequenztechnik und Elektronik,
Kaiserstr. 12, 76131 Karlsruhe, Germany
Email: manfred.thumm@ihm.fzk.de

H. Braune, V. Erckmann, F. Hollmann, L. Jonitz, H.P. Laqua, G. Michel, F. Noke, F. Purps, T. Schulz, M. Weissgerber
Max-Planck-Institut für Plasmaphysik (IPP),
Wendelsteinstr. 1, 17491 Greifswald, Germany

P. Brand, M. Grünert, W. Kasparek, H. Kumric, C. Lechte, B. Plaum
Institut für Plasmaforschung, Universität Stuttgart,
Pfaffenwaldring 31, 70569 Stuttgart, Germany

Abstract: Electron cyclotron heating (ECH) has proven to be one of the most attractive heating schemes for stellarators, as it provides net current free plasma start up and heating. Both, the stellarator Wendelstein 7-X (W7-X), which is under construction at IPP-Greifswald, Germany, and the ITER tokamak, which will be built at Cadarache, France, will be equipped with a strong EC-heating and current drive system. Both systems are comparable in frequency and have CW (continuous wave) capability (0.14 THz, 10 MW for W7-X and 0.17 THz, 24 MW for ITER). The commissioning of the ECH plant for W7-X is well underway, the status of the project and first integrated full power test results from two modules are reported and may provide valuable input for the ITER plant. The 10 gyrotrons at W7-X will be arranged in two sub-groups symmetrically to a central beam duct in the ECH hall. The RF-wave of each subgroup will be combined and transmitted by a purely optical multibeam wave guide transmission line (copper mirrors) from the gyrotrons to the plasma torus. The combination of the 5 gyrotron beams to two beam lines each with a power of 5 MW reduces the complexity of the system considerably. The single-beam as well as the multi-beam waveguide mirrors and the polarizers have been already manufactured. Cold tests of a full size uncooled prototype line delivered an efficiency exceeding 90%. The mm-wave power will be launched to the plasma through ten synthetic-diamond barrier windows and in-vessel quasi-optical plug-in launchers allowing each 1 MW RF-beam to be steered independently. The polarization as well as the poloidal and toroidal launch angle will be adjusted individually to provide optimum conditions for different heating and current drive scenarios. The first series gyrotrons were tested and yielded a total output power of 0.98 MW, with an efficiency of 31% (without a single-stage depressed collector) in short-pulse operation and of 0.92 MW in pulses of 1800 s (efficiency of almost 45% at a depression voltage of 29 kV). The Gaussian mode output power was 0.90 MW and the power measured in a calorimetric load after a 25-m-long quasi-optical transmission line (seven mirrors) was 0.87 MW.

Keywords: Electron cyclotron heating, Fusion plasmas, Stellarator, High power CW gyrotron, Quasi-Optical transmission.

doi: 10.11906/TST.073-099.2008.06.09

1. INTRODUCTION

The physics goals of the W7-X stellarator experiment at IPP Greifswald, Germany, determine the main machine parameters as well as the choice of heating systems, diagnostics, data acquisition and machine control. W7-X (R = 5.5 m, a= 0.55 m) is the next step in the stellarator approach towards magnetic confinement fusion power plants. In contrast to tokamaks, stellarators have inherent steady state operation capability, because the confining magnetic field is generated solely by external coils.

The scientific objectives of W7-X can be summarized as follows:

(1) Demonstration of quasi steady state operation at fusion reactor relevant plasma parameters

(2) Demonstration of good plasma confinement

(3) Demonstration of stable plasma equilibrium at a reactor relevant plasma pressure parameter ß of about 5 %

(4) Investigation and development of a helical divertor to control plasma density, plasma energy and impurities.

W7-X will be equipped with a superconducting coil system, a continuously operating plasma heating system and an actively pumped divertor for stationary particle and energy control. The outline design is shown in Fig.1. In contrast to ITER, W7-X does not aim at DT-operation and provisions for remote handling in a radioactive environment are not foreseen. ECH will be the main heating scenario for steady state operation. The high-ß discharges will be investigated in pulsed experiments (< 10 s) at reduced magnetic field in a later state of the machine operation, when neutral beam injection heating will be available at a power level of 20 MW for 10 s.

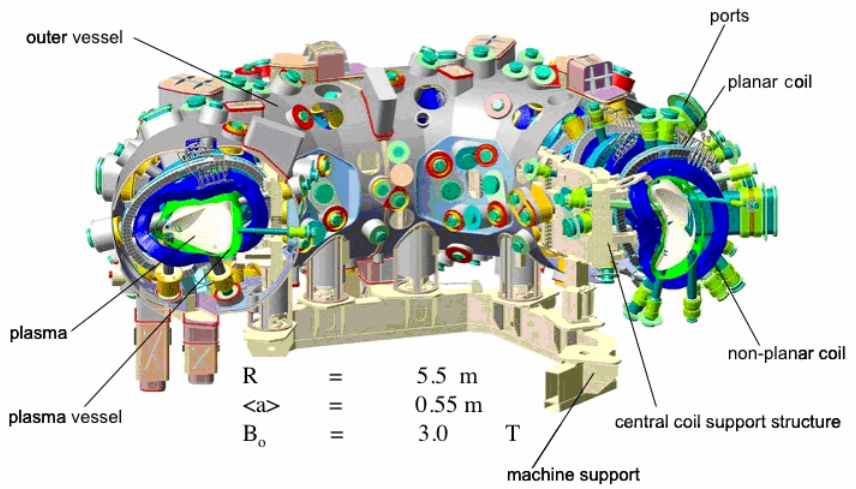

Fig. 1 The W7-X stellarator at IPP Greifswald.

An EC-heating power of 10 MW is required to achieve the envisaged plasma parameters [1] at the nominal magnetic field of 2.5 T. The standard heating and current drive scenario is in the 2nd harmonic extraordinary mode (X2) with low field side launch. High-density operation above the X2 cut-off density at $1.2 \cdot 10^{20}$ m^{-3} is accessible with the 2nd harmonic ordinary mode (O2, ne $< 2.5 \cdot 10^{20}$ m^{-3}) and at even higher densities with O-X-Bernstein-wave (OXB) mode conversion heating [2,3]. Theoretical investigations show, that 3rd harmonic extraordinary mode (X3) heating (B_{res}= 1.66 T, $n_e < 1.6 \cdot 10^{20}$ m^{-3}) is a promising scenario for operation at reduced magnetic field, and would extend the operation-flexibility further. The W7-X magnetic configuration minimizes plasma net currents, such as the pressure-driven bootstrap current. Residual bootstrap currents are expected to be small and will be in

the range up to 20 kA. As W7-X has no OH transformer for inductive current compensation, ECCD employing steering mirrors is a good candidate to counteract residual plasma net currents and thus to control the rotational transform. The predicted plasma parameters have been calculated with a new ray-tracing code and a new transport code for a conservative and a more optimistic approach [4]. The ray-tracing code was also used to optimize the ECH-launcher and the related in-vessel structures to satisfy the different demands for all proposed operation scenarios. The resulting technological solutions are presented in Section III. The total ECH power will be generated by 10 gyrotrons operating at 0.14 THz with 1 MW output power in CW operation each. The construction of the ECH-system is in a well-advanced state, the general design features and the status of both the gyrotron and transmission line commissioning is presented in Section II. Recent results from high power performance tests for most of a single system are presented in Section III.

The physics demands for both, W7-X and ITER request a versatile and flexible 'day one' ECH-system with high reliability. Some basic features of both systems are compared in Table 1, the similarities are obvious with the ITER installation having more than twice the power.

	W7-X	ITER
Power (MW)	10	24
Power per Gyrotron (MW)	1	1 (2)
Frequency (THz)	0.14	0.17
Operation Mode (standard)	2nd harm. (2.5 T) CW (1800 s)	1st harm. (5.6 T) CW (1000 s)
Transmission	optical	waveguide
Launcher	front steering/ remote steering	front steering/ remote steering
Physics Demands	bulk heating and current drive q-profile shaping Net-current suppression	bulk heating and current drive q-profile shaping MHD-control Net-current enhancement

Table 1 ECH for W7-X and ITER, main parameters

2. THE ELECTRON CYCLOTRON HEATING SYSTEM

The design of the ECH-system took full advantage of the fact, that the ECH-building could be built exactly to fulfill the needs of ECH as seen in Fig. 2. The 10 gyrotrons operating at 0.14 THz (plus two optional tubes at 70 GHz for plasma start up at low magnetic field) and the auxiliary systems (high-voltage supplies, water cooling, liquid helium and liquid nitrogen supplies for the gyrotron magnets) will be placed in a separate ECH building adjacent to the central W7-X experimental hall.

The gyrotrons will be installed in two rows symmetrically to a central underground beam duct, which

connects the ECH hall with the stellarator hall. To achieve maximum reliability and availability, we have chosen a modular design, which allows commissioning and operation of each gyrotron and the required subsystems independently from all others. Maintenance or repair of one module is possible without affecting the operation of all other gyrotrons. This design also minimizes the costs because series production of identical modules is possible. It is evident from this concept, that the demonstration of CW-operation at full power with a single module, which was achieved recently, gives high confidence in the full system capability. An optical mm-wave transmission system was developed for W7-X, which is a simple, reliable and cost effective solution for a plasma device without DT-operation. The transmission of the RF-power to the torus (typically 60 m) will be performed by two open multi-beam mirror lines, each of them combining and handling 5 (+1) individual RF-beams (6 MW). The power handling capability has inherently a large safety margin (factor of 2-3) due to the low power density on the reflector surfaces. The maximum power density in the RF-beam is 0.16 MW/cm^2 (in the beam waist outside the gyrotron output window). This keeps the option open to replace the 1 MW gyrotrons by more powerful ones in a later state, if such gyrotrons become available. It is worth noting, that the W7-X transmission system satisfies the ITER-ECH (24 MW) power capability demands without modification at a somewhat lower safety margin. An underground concrete duct houses the individual components of the transmission system, the concrete walls are an efficient absorber of stray radiation from the open lines thus satisfying the safety-requirements on microwave shielding. All mirrors in the beam duct are remotely controlled.

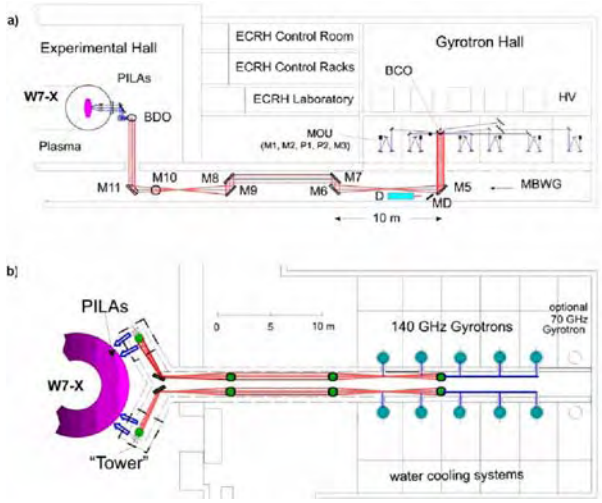

Fig. 2 Schematic design of the 0.14 THz/10 MW ECH-system for the stellarator W7-X:
a) side view b) top view

2.1. The W7-X Gyrotrons

The development of CW-gyrotrons with an output power in the megawatt range for thermonuclear plasma fusion applications was and still is subject of a worldwide R&D effort, which is mainly driven by the needs of the two large fusion devices W7-X and ITER.

(1) Gyrotron Design: The development of the 'W7-X gyrotron' started in 1998 in Europe with Thales Electron Devices (TED) in collaboration with EU Fusion Associations (FZK Karlsruhe, IPP Greifswald,

CRPP Lausanne, CEA Cadarache) and in the USA with CPI as industrial partners. Some important design parameters for both development lines are summarized in Table 2. The design approach for both gyrotrons includes single-stage collector depression (SDC) to enhance the efficiency and relax the collector loading. Both are 'diode-type' gyrotrons without a control anode (modulation anode) to simplify the design. The collector is at ground potential, the depression voltage (cavity and body) has positive, the cathode voltage has negative polarity, respectively. The output vacuum window [5] uses a single edge-cooled disk of chemical vapor-deposited diamond (CVD-diamond) with an outer diameter of 106 mm, a thickness of 1.8 mm (four half wavelengths) and a window aperture of 88 mm. The gyrotron cavities operate in the $TE_{28,8}$ mode (TED) and $TE_{28,7}$ (CPI), respectively.

	TED	CPI
RF output power (MW)	1	
Frequency (THz)	0.14	
Pulse duration	CW (30 min)	
Power modulation (kHz)	< 10	
Accelerating voltage (kV)	81	82
Collector depression voltage (kV)	27	< 30
Beam current (A)	40	< 45
Cavity mode	$TE_{28,8}$	$TE_{28,7}$
Efficiency (%)	45	> 40
Cavity radius (mm)	20.48	19.26
Quality factor ("hot")	1100	1130
Cavity magnetic field (T)	5.56	5.43
Launcher taper (mrad)	4	
Launcher efficiency (%)	98	
Window aperture (mm)	88	

Table 2 Design parameters for the TED- and CPI-gyrotron

Results of the two R&D tubes from TED are reported in [6] and results of the R&D at CPI are reported in [7-9], respectively.

The cavity design for the TED gyrotron features a linear input taper and a non-linear output taper. Self-consitent calculations including cavity thermal expansion and deformation result in a "hot" quality factor of 1100. Special care has been taken for the design of the quasi-optical mode converter [10] to minimize the generation of stray radiation. The radius of the antenna waveguide launcher is slightly up-tapered towards the output by an angle of 4 mrad in order to avoid parasitic oscillations in this region. Due to the low fields along the edge of the helical cut, this advanced dimpled-wall launcher [10] generates a well-focused Gaussian-like field pattern with low edge-diffraction. In combination with a three-mirror system the desired Gaussian output beam pattern is obtained, an example is shown in Fig.3.

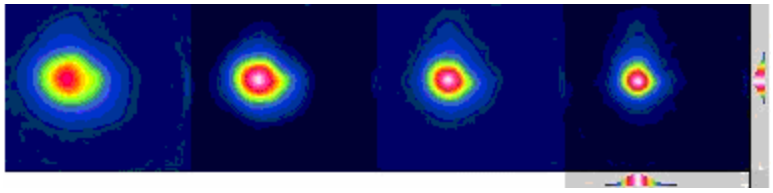

Fig. 3 Power distribution of the RF-beam at different distances from the gyrotron window (from the left: 1282 mm, 1082 mm, 882 mm and 682 mm).

The RF-power distribution was measured using an infrared (IR) camera and a PVC plate perpendicular to the output RF-beam direction at different positions with respect to the window. The pulse duration was 2-7 ms leading to a center temperature of about 60 °C for all distances. A Gaussian mode content of 97.5 % of the output beam was calculated from the these four measured patterns employing our phase retrieval and mode analysis code.

(2) Gyrotron Experiments: With the prototype gyrotrons in the TED-development line, two problems were faced: The specified output power of 1 MW was not completely achieved, which was attributed to an azimuthally inhomogeneous cathode emission. Furthermore the pulse duration was limited to about 15 minutes even at reduced power of 0.534 MW due to an increase of the internal gas pressure [11,12].

To eliminate these limitations, an improved quality assurance of the emitter ring (electron gun) was established before installing it into the gyrotron. Emitter surface quality and temperature homogeneity have been carefully checked. To avoid the pulse length limitation by the pressure increase in the tube (due to heating of the internal ion getter pumps by RF stray radiation), external ion getter pumps (IGP) were implemented in the design with improved RF stray radiation shielding. The R&D phase with TED was then terminated in 2002, followed by a commercial contract for 7 additional TED series gyrotrons. Together with both R&D-tubes and the CPI-gyrotron, all sockets of the ECH-plant will be equipped.

All TED-gyrotrons are pre-tested in the test facility at FZK prior to shipment to IPP, where they undergo the final full performance tests. TED-gyrotron S.No.1 showed an almost linear dependence of output power versus beam current at constant magnetic field. The saturation in power as measured in the prototype was absent indicating an improved quality of the electron beam. An output power of 1 MW at 40 A and 1.15 MW at 50 A was measured in short pulse operation (ms). The corresponding efficiencies without depressed collector were 31% and 30%, respectively [13].

All gyrotrons under test show a frequency chirp of typically 300 MHz during the first couple of seconds due to frequency pulling, space charge neutralization and heating and expansion of the cavity. The optimization of the operating parameters at high output power in 1 s-pulses was performed assuming that the instantaneous power is well described by the frequency difference between the initial frequency (cold cavity) and the instantaneous frequency (after one second). In a range between 5.52 –5.56 T of the cavity magnetic field, a slight power increase was measured with increasing magnetic field rather than a maximum for the output power. In order to achieve the maximum output power, the accelerating voltage (this corresponds to the energy of the electrons inside the cavity) was adjusted and followed nicely the law that the ratio between magnetic field and the relativistic factor γ has to be constant. Increasing the voltage beyond this value leads to an excitation of unwanted neighbouring modes. The measurements were performed at a constant beam current of 40 A and an optimized

electron beam radius inside the cavity.

A strong dependence of the output power on the electron beam radius in the cavity was found. The desired mode can only be excited in a narrow range between 10.25 mm and 10.43 mm. At lower beam radii, arcing occurs, at higher radii a wrong mode is excited. The optimum value of the beam radius decreases slightly with decreasing cavity field and beam current.

In long pulse operation up to 3 minutes, which is the test stand limit at FZK for a beam current > 30 A, the power was measured calorimetrically in an RF-load. The RF-beam is directed and focused by two matching mirrors and two polarizers into the load, which is located at a distance of about 6 m from the gyrotron window. The polarizers generate a circularly polarized wave to homogenize the power loading on the surface of the load. The first matching mirror possesses a grating surface, which directs a small amount of the RF-beam towards a horn antenna with a diode detector to get a power proportional signal. The gyrotron was operated with a typical depression voltage in the range 25-30 kV to limit the collector loading and optimize the efficiency. Fig. 4 displays some gyrotron operating parameters for a pulse length of three minutes. The electron beam current I_{beam} drops somewhat at the beginning of the pulse due to beam emission cooling of the electron gun and recovers on a slow inherent timescale (50 s) while boosting the heater power properly. The IGP current (tube pressure) shows some changes also, but on a very low level. The increase of pressure is less than a factor of two and stays well in the 10^{-9} mbar range. The highest measured directed power inside the load for a three-minute pulse was 0.91 MW. Including the external stray radiation, which was determined by calorimetric measurements inside the microwave chamber, the total gyrotron output power was 0.92 MW with an efficiency of almost 45 %. Thus the specified value of > 0.9 MW for the power in the fundamental Gaussian mode has been achieved. No arcing in the quasi-optical transmission line has been observed.

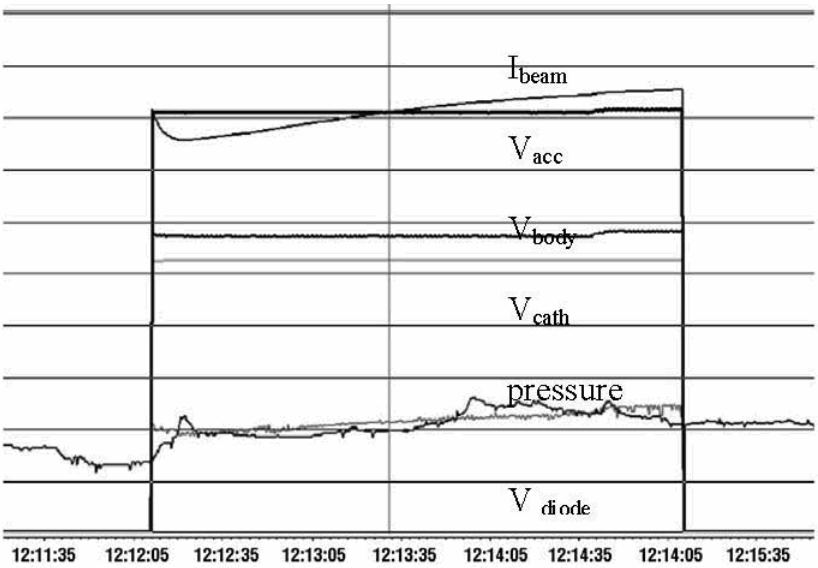

Fig. 4 Operation parameters vs. time (h:min:sec) of the TED gyrotron S.No.1 for 3 min pulse duration. From top to bottom: beam current (I_{beam}), accelerating voltage (V_{acc}), body voltage (V_{body}), cathode voltage (V_{cath}), diode signal (V_{diode}) and pressure monitor (vacuum). Ordinate scales are arbitrary.

After the successful tests at FZK, the tube was delivered to IPP Greifswald for final tests in 30 minutes operation and the year 2005 saw the successful full performance tests of gyrotrons from both

manufacturers, TED and CPI at IPP. Fig. 5 shows the TED gyrotron in its superconducting (SC) magnet in the installation at IPP Greifswald.

Fig. 5 The TED S.No.1-gyrotron at IPP Greifswald.

Typical time traces of the output power and the gyrotron pressure (IGP-current) for an experimental sequence of one shorter (5 min) and one long pulse (30 min) are shown in Fig. 6. The slow rise and fall times of the RF-power trace is determined by the characteristic time constant of the CW-calorimeter. The small steady increase of the gyrotron pressure as seen from Fig. 6 (bottom) indicates, that the tube has not yet reached steady state after 30 min, although all other measured parameters became stationary. Power modulation was demonstrated up to 20 kHz by modulating the body voltage [14]. An almost linear dependence of the output power on the body voltage was measured. The RF-power versus acceleration voltage characteristics for the CPI-gyrotron is plotted in Fig. 7 (top) for 10 min pulses [4]. It provides a very convenient voltage range for the power control.

An example for a beam-current scan for TED-gyrotron S.No.1 is shown in Fig. 7 (bottom), each data point was taken in pulses with 1-5 min pulse duration. The scan was performed up to a maximum output-power of 0.96 MW with an efficiency of 44 %, indicating the full gyrotron capability. We have chosen somewhat more conservative parameters for the 30 min operation, which is the target plasma discharge length of the stellarator W7-X. The gyrotrons were operated at a power in the directed beam of about 0.9 MW (CPI) and 0.92 MW (TED), the related power measured in the calorimetric CW-load was 0.83 MW (CPI) and 0.87 MW (TED). Note, that due to the inherent mode filtering capability of an

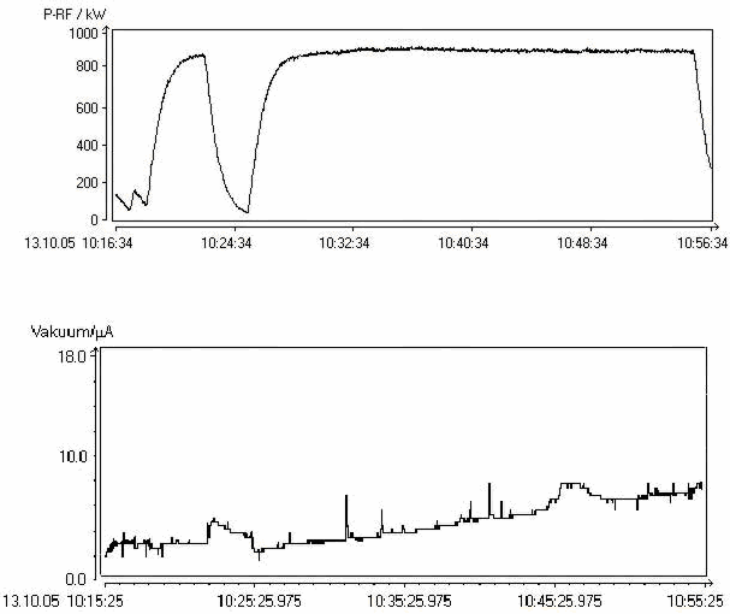

Fig. 6 Example of a 30 min shot of the TED gyrotron S.No.1 (with a 5 min shot as precursor). RF-power (top) and gyrotron vacuum (IGP-current, bottom) as a function of time (h:min:sec).

optical beam waveguide only the Gaussian mode content of the gyrotron beam reaches the CW-load. The total transmission losses after seven mirrors were estimated in the range 50-70 kW. Since the Gaussian mode purity of the CPIgyrotron was not known with the required accuracy, slightly higher losses (70 kW) resulting from an imperfect Beam-Matching-Optics (BMO) unit had to be accepted as compared to the TED-gyrotron (50 kW). The CPI-gyrotron opened a collector vacuum leak after having passed the acceptance test and was returned to the manufacturer for repair. The TED gyrotron S. No. 1 was mothballed after the acceptance tests.

At present, 4 out of the 10 units of the ECRH-system are operational and further commissioning is in progress.

1 MW output power has also been achieved with S.No.2 and S.No.3. However, with both tubes it was not possible to increase the pulse length and to find parameters of good performance. To avoid competition with the parasitic $TE_{27,8}$ mode the beam voltage had to be reduced to low values which resulted in unacceptable power and efficiency of S.No.2 and S.No.3.

The dependence of the output power on the accelerating voltage is shown in Fig. 8 for S.No.3 in short pulse operation (3 ms). The output power has been measured for different combinations of the cavity magnetic field and beam radius in the cavity, the beam current was 41 A – 44 A. However, at longer pulses (1 s) the performance of S.No.3 was similar to S.No.2 and the maximum achievable output power was considerably reduced (0.65 MW in pulses of 3 min).

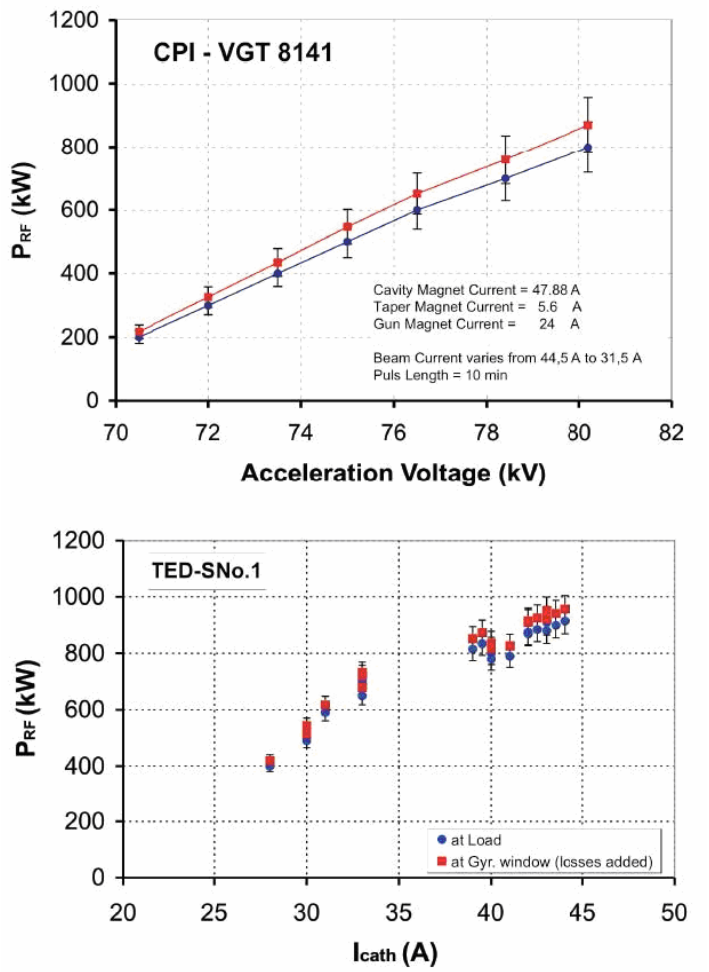

Fig. 7 Top: Output power (squares) and RF-power to load (dots) as a function of the acceleration voltage for the CPI-gyrotron. Bottom: Same quantities as a function of the beam current for the TED-gyrotron S.No.1.

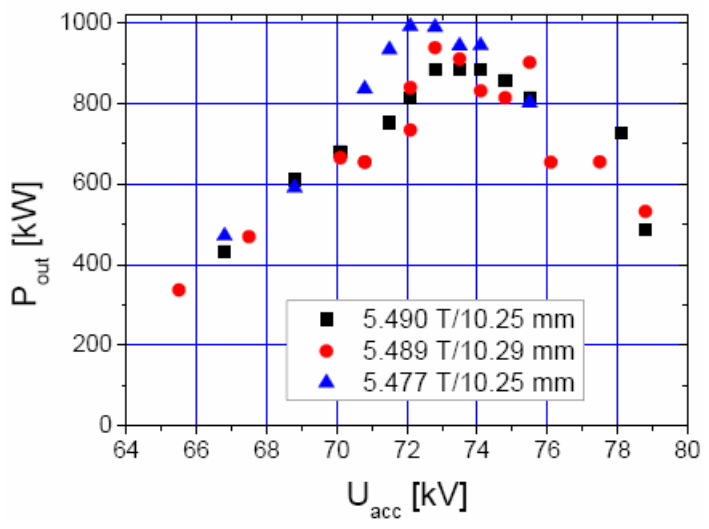

Figure 8 Output power of TED-gyrotron S.No.3 vs. accelerating voltage for different combinations of cavity magnetic field and electron beam radius in the cavity.

Both gyrotrons have been opened and subjected to a visual inspection. It was found that in the beam tunnel, close to the entrance of the cavity, several brazes of the absorbing ceramic disks and the disks themselves were defective. Cracks at the interface metal/ceramics and through the ceramics were observed. The inspection indicates that there were several locations with high temperature of the ceramic material.

In the meantime TED-gyrotron S.No.4 (with good beam tunnel) was tested at FZK and delivered identical parameters like S.No.1 (0.92 MW, 3 min, efficiency close to 45% and 97% mode purity). The tube is currently being tested for full performane 30 min at IPP Greifswald and the repaired S.No.2 at FZK.

The measured Gaussian mode purity of the output beams of TED-gyrotrons No. 2, 3 and 4 is about 97% and comparable to S.No.1. The repaired gyrotron S.No.3 is close to completion in the factory.

(3)Optimization of Gyrotron Collector Loading: State-of-the-art MW-class CW-gyrotrons operate with an efficiency of typically 40 -50 %. Thus 1-1.5 MW power remains in the electron-beam after the electron-wave interaction and must be dissipated in the collector. Vertical magnetic field sweeping systems (VFSS) became a standard technique, which keeps the time averaged specific heat dissipation at the collector within technically acceptable limits (<5 MW/m^2). As such collectors operate close to the technological limits, they represent a high-risk component with a small safety margin and often infer a power limit to gyrotron operation. To address this problem we have used the existing experimental set-up with an industrial TED gyrotron to investigate and optimize the power distribution of the electron beam along the collector surface. The vertical beam spread (FWHM) without sweeping is about 50 mm, leading to a power density at nominal operation of about 20 MW/m^2, which is unacceptably high. All TED gyrotrons thus are equipped with a VFSS running at an optimized sweep frequency of 7 Hz. A broad power deposition profile with strong peaking at the upper and lower turning points of the beam is achieved as plotted in Fig. 9.

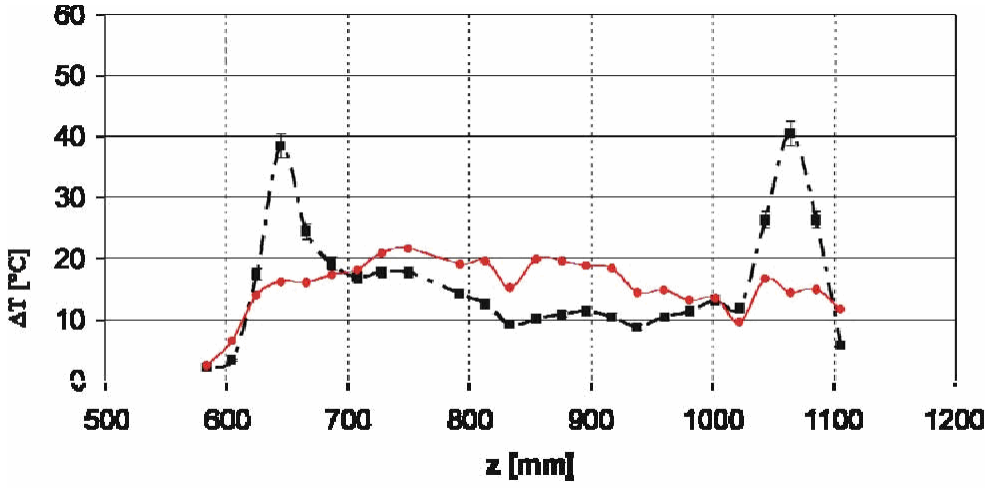

Fig. 9 Profiles of the gyrotron collector temperature increase ΔT along the vertical coordinate z for combined collector sweeping (dots). The profile for VFSS only is also shown for reference (squares).

The measurements are taken with an array of 49 thermocouples mounted at equal distances along the

vertical direction of the collector. The temperature rise is measured as a function of vertical distance for the optimum sweep parameters. IR camera measurements showed that the temperature distribution is almost azimuthally symmetric. In principle, the power peaking could be avoided by running a saw-tooth like waveform. The AC-magnetic field, however, is strongly shielded by the copper cylinder of the collector, which affects particularly the higher Fourier harmonics and only the low frequency components can penetrate.

In a first step, we have performed experiments with a rotating transverse field sweeping system (TFSS). The TFSS consists of 3 pairs of TF-coils (Fig. 10), which are powered by a simple 3-phase AC-supply thus generating a transverse field, which rotates with 50 Hz [15]. The measurements were performed with reduced e-beam parameters (typically 15 A, 50 kV). The power peaking remained in the lower collector area and no advantage was gained with respect to the collector loading limits. However, the increased sweeping frequency significantly reduces collector fatigue. In a next step, we have combined both, the TFSS and the VFSS. By proper tuning of both systems an almost perfectly flat power deposition profile along the collector area was obtained as demonstrated in Fig. 9 [16]. A small DC-component was superimposed to control the position of the lower turning point. The peak loading is reduced by about a factor of 2 as compared to VFSS alone, which increases the safety margin of the present collector design significantly and/or may allow operation of the TED series tubes at higher electron beam currents (and possibly higher output power).

Fig.10 The TED-gyrotron collector with three pairs of TF-coils (the VF-coil is removed)

2.2. The Quasi-Optical Transmission System

(1) The Multi-Beam-Waveguide: For high-power transmission of millimeter waves, free-space beam waveguides as well as highly oversized corrugated waveguides are in use [17]. Owing to good experiences with a 0.8 MW / 0.14 THz beam waveguide on the stellarator W7-AS, a quasi-optical transmission system was chosen for W7-X [18]. Here, the mm-waves are transmitted as Gaussian beam by successive transformation with metallic mirrors [19,20]. The standard mirror design employs ellipsoids where the foci are determined by the phase centers of the incident and the reflected beam, respectively [21]. This shape gives minimum conversion to higher order modes [22]. Mirror shapes for astigmatic beams (as used for the matching of the gyrotron to the transmission line) are discussed in [23].

The main advantages of this concept are the low (ohmic and diffractive) losses, the high power capability due to relatively low field strength and the inherent mode filtering as high order modes are diffracted out of the system. A major disadvantage of beam waveguides is the diameter of the beam and thus the size of the mirrors governed by the spacing of adjacent mirrors and the lateral expansion of the beam along propagation. Therefore systems with several channels are generally complex and bulky.

To overcome this disadvantage, a Multi-Beam Waveguide (MBWG) was developed for the ECH transmission to W7-X. Here, many quasi-optical beams are transmitted by a common mirror system. Basically, the MBWG consists of four focusing mirrors in a confocal arrangement, and must simultaneously offer a low-loss propagation of all (on-axis and off-axis) beams in combination with a correct imaging of the beam positions from the input to the output plane. The principle is illustrated in Fig. 11, where one unit consisting of 2 mirrors in Z-configuration is sketched: The waists of the beams are located at the input plane (located at a distance f in front of the first mirror), and the beams are injected parallel to each other into the common mirror system. Behind the first mirror, all beams cross in its focal plane. Behind the focal plane of the second mirror, the beams are parallel again, and the beam configuration injected at the input is recovered. The central (on-axis) beam will have a frequency of 0.07 THz, which requires the full mirror surface due to the larger beam divergence at the longer wavelengths.

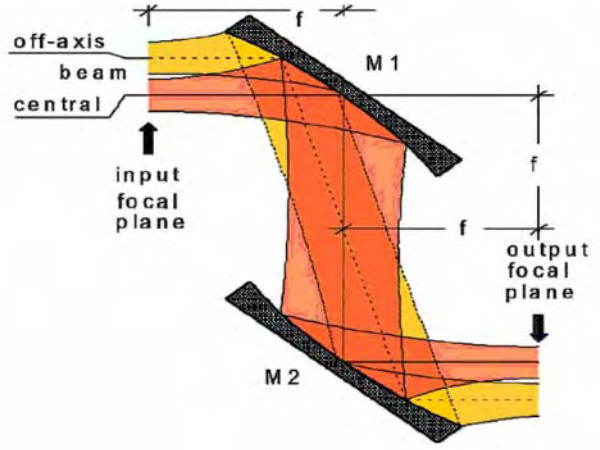

Fig.11 Principle set up of a confocal 2-mirror multi-beam waveguide in Z-configuration

To optimize the mirror shapes and to find the best arrangement of the mirrors, diffraction calculations with Gaussian beam mode analysis were performed [24]. Note that for a compact MBWG design, the individual beams overlap on the mirrors, so that no optimization of corresponding sections of the mirror surfaces is possible.

The study showed, that simple toroidal mirrors are the best compromise between the ellipsoidal shape required for optimum Gaussian beam transmission and the paraboloidal shape for best imaging characteristics. An essential parameter is the mirror arrangement: out of the 8 possible arrangements for the four mirrors, only two (Z-configuration and square configuration) give optimum performance [24]. For these two configurations, the spurious modes which are excited on each mirror surface destructively interfere after four mirrors, and the beams cross the output plane exactly perpendicular in the nominal position. For the parameters of W7-X, the matching coefficient between input and output is 99.9%. With the finite size of the mirrors taken into account, the transmission efficiency in the nominal mode is >99.5 % (without Ohmic losses). Further calculations show, that even a much higher number of beams could be transmitted via a common mirror system without remarkable diffraction loss.

(2) Design of the Optical Transmission System: The general arrangement of the transmission system is sketched in Fig. 2. The gyrotrons, which are installed behind the concrete walls of the underground beam duct radiate their power laterally through holes in the duct walls. For each gyrotron, a beam conditioning optics consisting of five single-beam mirrors is used. One Single Beam Waveguide (SBWG) module is shown in Fig. 12 together with additional components such as short-pulse calorimeter, RF-shielding elements and switch mirrors. The beam combining optics (BCO) module is also seen in the background. Two SBWG-mirrors (M1 and M2) match the gyrotron output to a Gaussian beam with the correct beam parameters. These mirrors are the only elements, which have to be adapted to the individual gyrotron RF-output beam and can be designed and built according to the delivery sequence of the gyrotrons without affecting the lay-out of the overall system. The following two plane reflectors (P1 and P2) are corrugated with a sinusoidal corrugation profile [25] to set the polarization needed for optimum absorption of the radiation in the plasma. The first of these polarizers (elliptical polarizer P1, groove period = 1.28 mm, depth = 0.56 mm), shifts the polarization between the TE and the TM wave by 90°, thus by rotation any ellipticity of the reflected radiation can be set. The second polarizer (period = 1.28 mm, depth = 0.78 mm) has a corrugation for a 180° phase shift to turn the axis of the polarization ellipse to the appropriate orientation. A fifth mirror (M3) directs the beam to a plane mirror array (BCO) at the input plane of the MBWG. This MBWG is designed to transmit up to seven beams (five 0.14 THz beams, one 0.07 THz beam plus an additional spare channel) from the gyrotron area (input plane) to W7-X (output plane). In addition to the four focusing mirrors, three additional plane mirrors are used to fit the transmission lines into the underground beam duct. A section of the two symmetrically arranged MBWG's is shown in Fig. 13.

Two mounting towers will house the mirror array (Beam Distribution Optics, BDO-module) at the output plane of the MBWGs, which separates the beams and directs them via two mirrors towards the plug-in launcher as shown in Fig. 14. The spare channel of the MBWGs will be used to switch one beam on each side from a standard low-field steering (LFS) launcher to a high-field steering (HFS) launcher in the N-port (which may be a remote steering launcher). The length of the MBWGs is 45 m, the total length of the transmission lines will be 57 to 65 m depending on the location of the gyrotron.

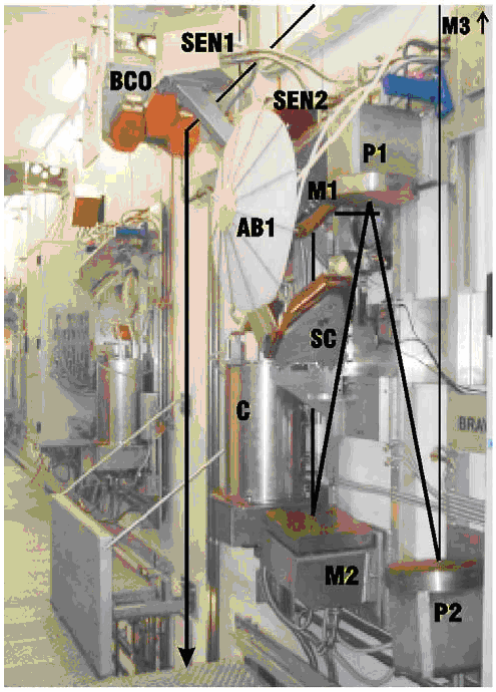

Fig. 12 Beam conditioning unit of channel B5 consisting of the matching mirrors M1 and M2, polarizers P1 and P2, and the calorimeter C with switching mirror SC. Stray radiation absorbers(AB1) are mounted behind M1 and inside the wall bore hole. M3 (not shown) guides the beam to the beam combining optics BCO. Mirrors SEN1 and SEN2 allow to switch the beam to transmission channel N serving the N-port for HFS launch.

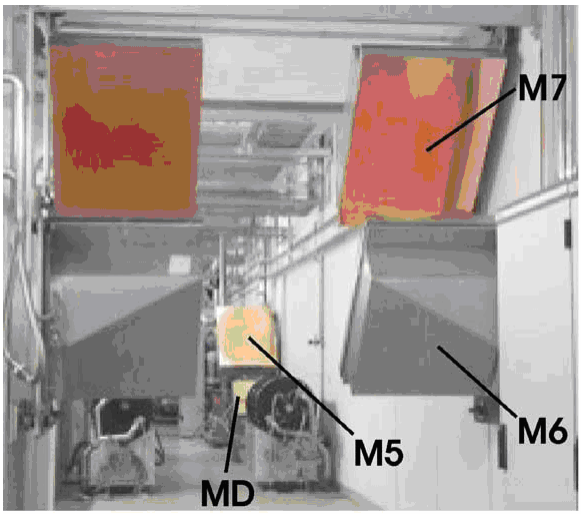

Fig. 13 View into the transmission duct showing the mirrors M6, M7 of the two MBWGs (foreground) and the MBWG mirrors M5 as well as the mirrors MD, which allow to transmit each individual beam into a calorimetric CW-load (background).

(3)Diagnostics for the Optical Transmission System: Power monitoring in the line is performed with grating couplers [26], which are embedded into the copper surface of M1. The coupled beam is either transmitted to a matched horn antenna or a bolometer. M1 is also equipped with temperature sensors and a flow meter for calorimetric measurement of the ohmic loss on the mirror to monitor the transmitted power. By switching the mirror SC (see Fig. 12) each gyrotron beam can be directed into the calorimetric load consisting of a double-walled cylindrical absorbing chamber with two layers of

water-cooled Teflon hoses at the inner wall. An optimized conical mirror distributes the radiation homogenously over the Teflon hoses, a socalled modified Winston cone [27] at the input reduces the reflections to about 1 %. The calorimeters are designed for a typical pulse duration of 0.5 s at full power.

By tilting one of the BCO mirrors, the corresponding beam can be steered via mirror MD into a commercial CW load (see Fig. 13). Since this load showed reflections of the order of several percent, a mirror with the shape of a rotational ellipsoid was attached at the input of the load, which reduces the reflected power significantly.

(4)Mirror Technology: All mirrors must maintain a stable surface under the heat loads imposed by the ohmic loss of the millimeter waves. The ohmic loss of different copper surfaces as used in the transmission line (plane; shallow diagnostic gratings; polarizing grooves) was measured with a 3-mirror resonator technique [28], the data were used as input for the mirror design and cooling concept. This results in losses of up to 3 kW per Megawatt beam with thermal loads of up to 100 W/cm2 on each mirror surface.

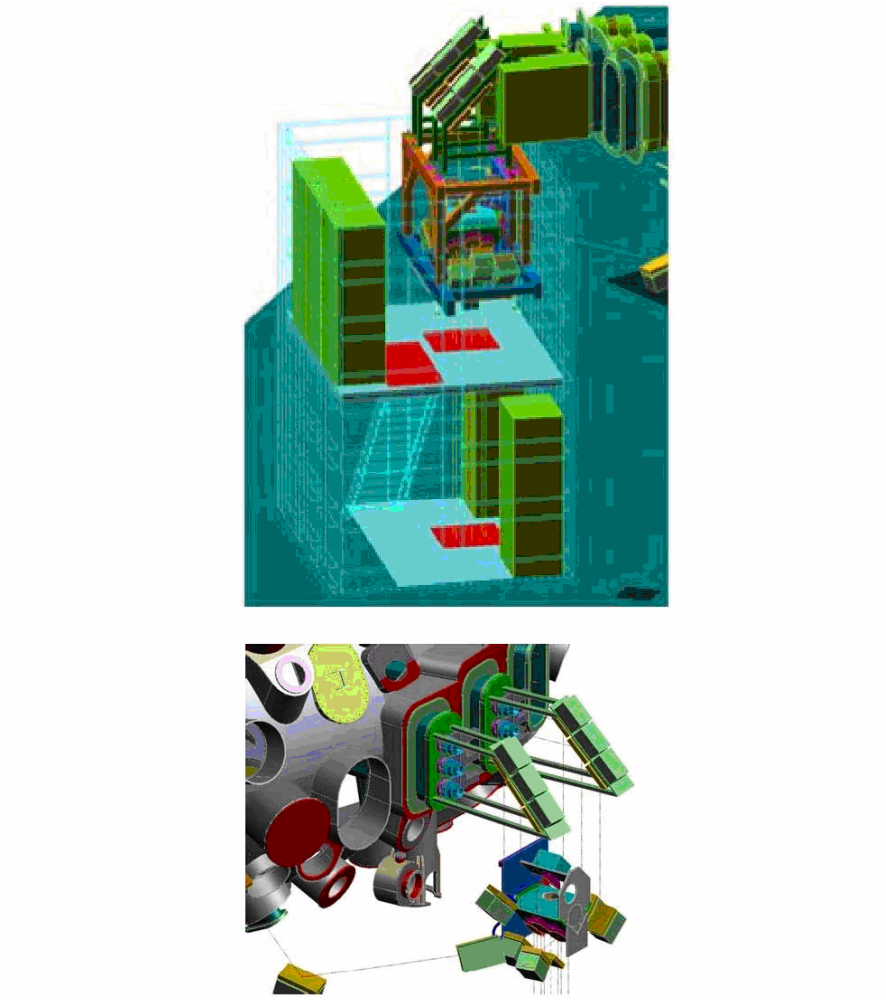

Fig. 14 Top: One of the ECH towers, which houses the BDO-module. Buttom: Detail of the mirror-arry in front of the equatiorial ports. The mirror for HFS-launch through a separate N-port is also seen

To minimize surface deformations due to thermal loads a 60 – 70 mm thick honeycomb structure from stainless steel with a thin (2 mm) layer of electro-formed copper on the mirror surface was chosen as seen from Fig.15. The cooling channels are in direct contact with the copper layer and spiral from the center (water inlet) to the edge of the mirror (water outlet).

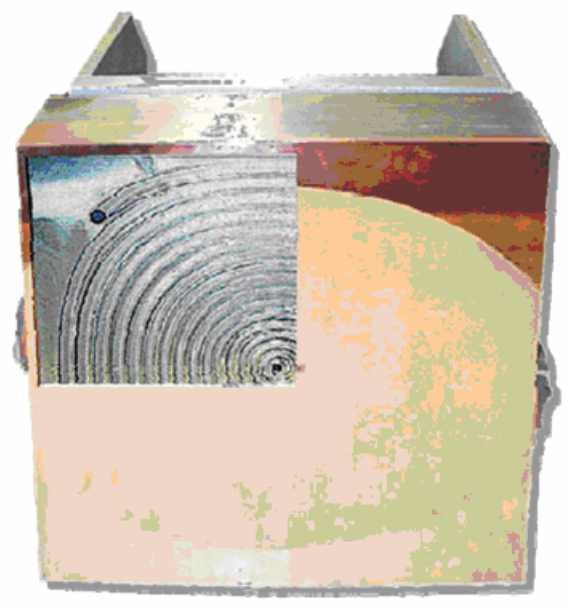

Fig. 15 Single beam mirror with the Cu-SS sandwich structure. The copper surface is partly removed to show the cooling channel spiral.

The width, the depth, and the number of the spirals is adapted to the different mirror shapes (rectangular, square, hexagon, circular) and dimensions (190 x 270 mm .... 740 x 1100 mm). The heat removal matches the local heat transfer to the Gaussian distribution of the heat load [29,30]. Even in the transient phase in the first minute after full power switch-on, the variation of the mirror curvature stays below 10^{-3} m^{-1}, which was confirmed experimentally. All mirrors are mounted on stable supports allowing two-axis adjustment by remote control.

(5)Alignment of the Mirror System: The mirrors are pre-aligned with lasers, final alignment is performed with the high-power beams using thermographic methods. If necessary, the alignment will be continuously checked by a system based on FM-reflectometry [31]. For this purpose, all mirrors have shallow phase gratings on their surface designed such that for correct alignment the -1st-order Littrow condition is fulfilled at a frequency of 0.188 THz. A low-power probing beam at this frequency which is coupled co-axially into the system will lead to reflected signals from the mirrors which are a measure for the quality of the alignment of the mirrors. A test of this scheme at the quasi-optical part of a 0.14 THz ECRH transmission line on W7-AS was successful and showed a spatial resolution of 0.15 m, which is by far enough to discriminate signals from the individual mirrors.

As alternative for the alignment control and power measurement in front of the torus window, a system based on a holographic grating coupler with conical scanning of the diffracted beam is in preparation [32].

2.3. Transmission Characteristics

(1) Transmission Efficiency and Mode Purity: The overall transmission efficiency is determined by ohmic dissipation in the mirrors, diffraction loss due to mode conversion and mirror surface deformation, beam truncation of the reflectors and windows, misalignment, as well as atmospheric absorption. The estimated contributions are listed in Table 3. One can see, that a total transmission efficiency of 90 % is expected for a pure Gaussian beam. Additionally, higher-order mode losses and stray radiation from the gyrotron output beam of typically 3 % are estimated which have to be absorbed by water-cooled absorbers and the concrete walls of the beam duct.

Loss channel	Number of elements	Loss
Absorption on mirrors	14 plane + 2 grooved Cu surfaces	2.5%
Diffraction and beam truncation	16 reflectors	2%
Misalignment	Transmission line	2%
Atmospheric absorption	60 m dried air	0.8%
Beam truncation, launcher	1 Window + 2 int. mirrors	3%
TOTAL LOSS		10%

Table 3 Contributions to the transmission loss for the ECH system on W7-X.

(2) Low-power Measurements of Transmission Efficiency and Mode Purity: Due to the complexity of the system and in order to test its over-all performance and stability, a full-scale prototype had been built. Amplitude and phase measurements of the beams have been performed at the characteristic planes using various field scanning devices together with a vector network analyzer. An example of the beam power and phase distributions for all transmission channels at the output plane of the MBWG (corresponds to the position of the BDO, see Fig. 2) is shown in Fig. 16. For each channel, the patterns show an almost rotationally symmetric amplitude distribution and only small variations of the phase (plane phase front in the beam waist) and thus demonstrate the good imaging characteristics of the confocal system even for off-axis beams. The mode analysis of the measured beam patterns at the exit of the multi-beam section yields a TEM_{00}-mode purity of more than 98 %. The total transmission efficiency of the complete prototype system (17 mirrors) was checked by calorimetric methods and yielded 90±2 %, which is in good agreement with the theoretical value.

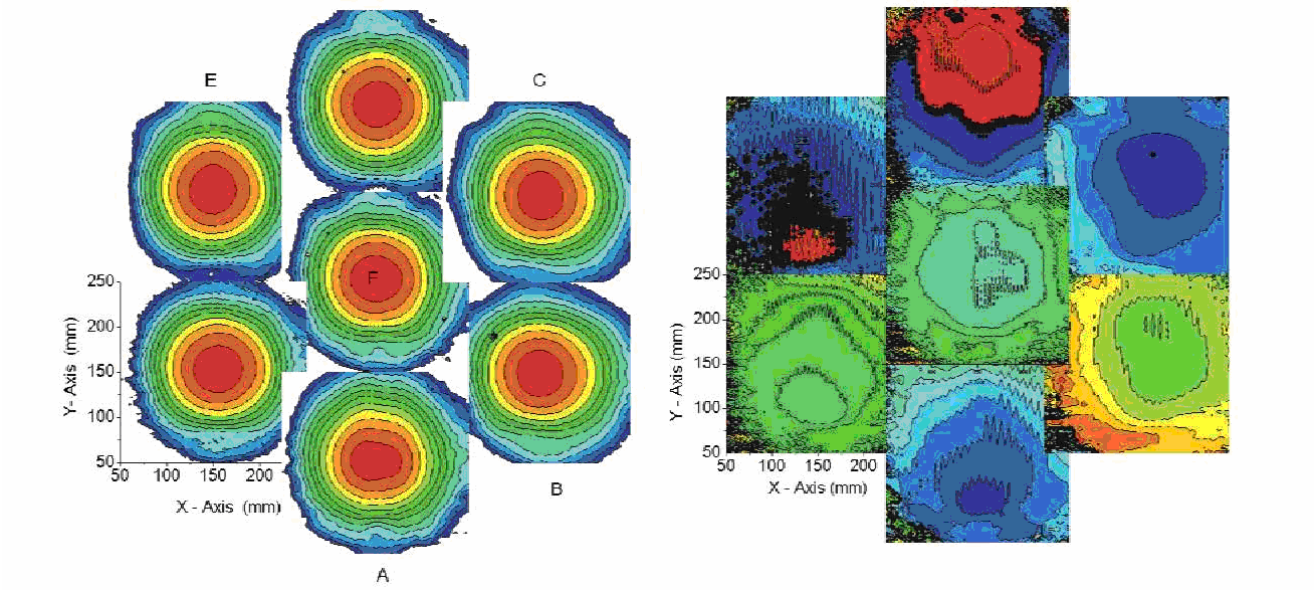

Fig. 16 Low-power measurements of power density (Scale: 3 dB/colour step), and phase distribution (20°/colour step) for seven RF-beams at the output plane of the MBWG..

(3) High-Power Measurements of Beam Parameters: The thermographic recording, phase retrieval and mode analysis of the output beams of several gyrotrons yielded a high TEM00 mode purity of ≥ 97%. Therefore, the matching mirrors M1 and M2 were designed as simple ellipsoidal mirrors, which only have to correct for the slight astigmatism of the gyrotron beam. At the end of the single-beam line in front of the dummy load (see Fig. 13), the intensity distribution of the beam was measured at several positions using thermography of a PVC target inserted into the beam path. The preliminary analysis of the data is plotted in Fig. 17, with the insert showing a typical beam pattern. As can be seen from the graph, the beam radii in vertical and horizontal direction are in good agreement with the calculated parameters of the circular Gaussian beam.

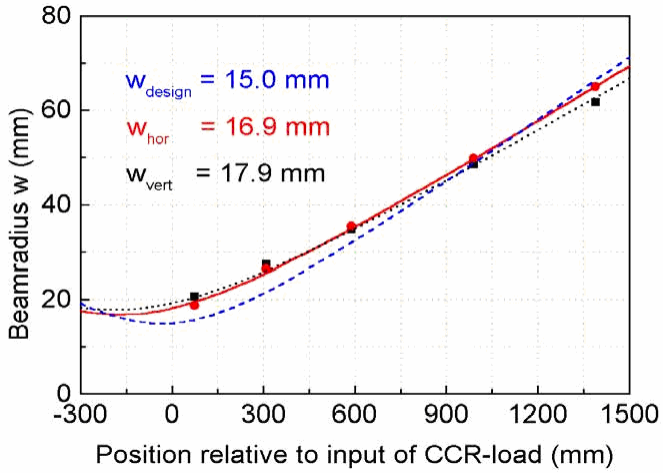

Fig. 17 RF-beam radii in horizontal (measurement: dots; fit: solid line) and vertical (measurement: squares, fit: dotted line) direction of the beam in front of the dummy load as deduced from thermographic images (see insert), and comparison with design (dashed line).

2.4. Integrated High-Power CW Test

The full performance tests were performed with both, the TED-and the CPI-gyrotron operating at an output power of about 0.9 MW for 30 minutes. The microwave beams were transmitted through 7 single beam mirrors of the transmission system into a calorimetric CW-load to perform integrated tests of two modules of the ECH plant. The data for CW-operation as presented in Section II.A were obtained in this set-up.

During high-power tests all mirrors performed well. In particular, no arcing was seen on the corrugated surfaces of the polarizers, which are considered the most critical (and most loaded) elements, provided that they were clean.

It is worth noting, that all peripheral systems at IPP Greifswald like main power supply, central cooling system, body-modulator, transmission line components, RF-diagnostics, as well as the central control and data-acquisition system are new and had to go through this integrated qualification process together with the gyrotrons.

Small side lobes of the RF-beam were hitting the beam duct concrete wall or weakly cooled elements like the first mirror-support and additional water cooled absorbing targets had to be installed at the measured hot spots to avoid overheating. It is expected, that some fraction of the lost power from the CPI-gyrotron will be recovered by an improved BMO, which would increase the useful power in the Gaussian mode. More important, however, is the reduction of the power in the beam side-lobes, which is already very small. Even a small fraction of directed power (some kW), which does not hit the water cooled transmission mirrors, may create hot spots and damage at weakly cooled surfaces in CW-operation. The more or less isotropic deposition of the small fraction of stray radiation is easily handled by the concrete walls and is of minor concern.

With the encouraging results from the integrated tests of two modules, series production and commissioning of the major system components were released and 5 modules are completed meanwhile.

The high-power, full performance, CW-tests reported here were restricted to the SBWG-section of the transmission line. For tests of the full distance transmission including the MBWG-section, a special optical arrangement with retro-reflectors mounted in the first image plane of the MBWG (i.e. at half distance of the MBWG (see Fig. 2)) is being prepared. This is a necessary intermediate step, because the optical elements in the torus hall can be installed and tested only in a late phase of the W7-X-torus assembly.

As seen from Fig. 18, the back-reflector is mounted on rails and on a turntable to reflect either one of the six beams, which are propagating forward in an outer channel of the MBWG, backward via the central channel. An additional movable mirror near to the entrance plane of the MBWG focuses the beam (also via mirror MD) into the CW-load.

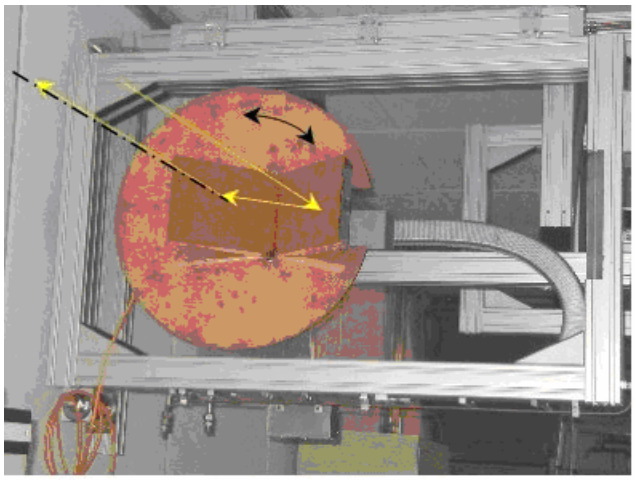

Fig. 18 Back-reflector mounted in the beam duct. The direction of the incident and reflected beam is indicated, the axis of symmetry (dashed dotted line) and the rotation direction is also sketched.

3. FRONT STEERING, LAUNCHER AND IN-VESSEL COMPONENTS

The various ECH and ECCD scenarios as discussed in [4] require a flexible launching system to cope with the demands for different mode-coupling. Furthermore, the high heat load conditions in CW-operation necessitate a reliable technical solution for the in-vessel components, which can sustain both, the power load of the microwaves and the plasma radiation. Several critical components have already been tested with respect to reliability and heat loading capability.

3.1. ECH Front Steering Launcher Development

Altogether 12 RF-beams (10 plus two spare ones) will be launched through 4 large equatorial ports (type A and E) for the LFS-launch scenarios. Three beam-lines will be stacked and incorporated into one plug-in launcher (PILA) as shown in Fig. 19 (top). Two out of the ten beam lines can be switched towards two lateral N-type ports for the HFS scenarios. Each of the equatorial beams will be quasi-optically transmitted through its individual synthetic diamond vacuum window towards a fixed focusing mirror and a bi-axially movable, plane steering mirror at the front end. Water-cooled tubular structures will screen the beams and serve as a rigid mechanical support for the front mirrors. Specially designed apertures inside the beam tubes will reduce backward transmission of reflected power. The movable mirrors enable a poloidal steering range of ±25° and a toroidal steering range between ±15° and ±35°, which is more demanding than the present ITER design. The cooling water of the front steering mirror is fed through two push-pull rods, which are used for the mirror steering. The joints of the push-pull rod system are bridged by tube spirals as shown in Fig. 19 (bottom). The joints are screened by additional copper half shells and the surrounding tube spirals against microwave and plasma radiation. Assumed parameters for the design are a microwave radiation level of about 500 kW/m^2 and a plasma reliability. In a test with 10000 full scan cycles the accuracy of the positioning was found to be 0.05°. The motor drive was also successfully tested in a magnetic field of up to 40 mT, which is expected at the final motor position near the stellarator. The most critical elements are the water-cooling tube spirals made of stainless steel tubes with 7 and 8 mm diameter and 1 mm wall

thickness. Due to the bi-axial mirror movement, they have to withstand both a bending angle of up to 45° and a torsion of 10°. The maximum tension was calculated by an analytic model, which was benchmarked by a cyclic test of a down-scaled spiral (reduced number of windings). Cyclic tests with 10000 cycles were performed with increasing bending angle until the critical tension was reached and the spiral was broken. Based on these results the spirals were designed with a safety margin of about two. They passed the 10000 –cycle, full range test successfully. The spirals were annealed to minimize the internal tension before assembly. For two types of the spirals the tube circular cross-section was optimized and pressed into an elliptical one to avoid the contact of neighboring winding at the maximum bending angle. The measured hydro-mechanical properties of the spirals require a water-cooling system with 16 bar pressure for the front mirror cooling. After the successful completion of the R&D for the rod-joint-spiral assembly, the parts were integrated into the mock-up launcher including all vacuum feed-through's for the water cooling, motor drive rods etc. and were tested in a special Microwave Stray Radiation Loading (MISTRAL) test facility (Fig. 20) [4].

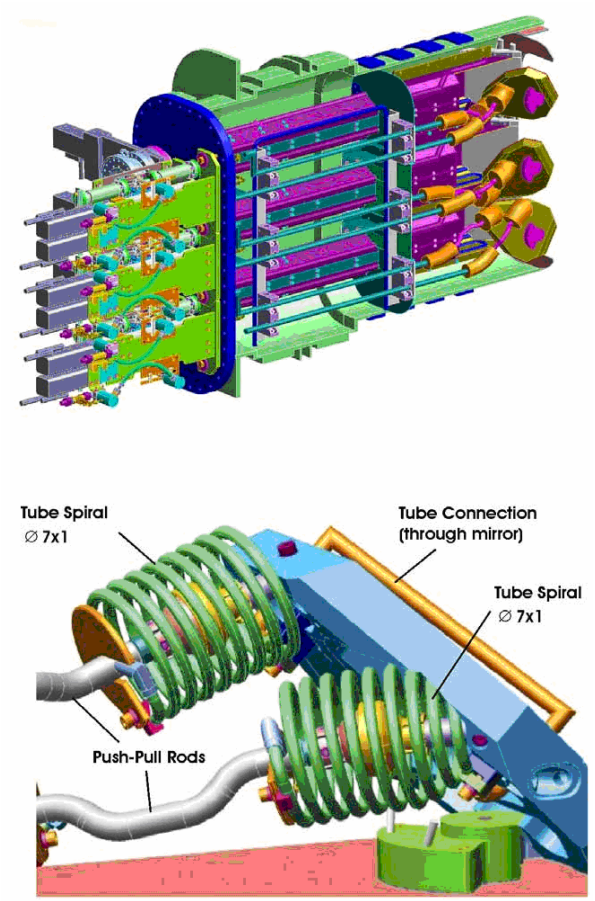

Fig. 19 ECH plug-in launcher for the equatorial port of the stellarator W7-X. Top: inside port design. Bottom: Mirror drive with push-pull rods and water-cooling spirals for the front mirror.

For the N-type port launch no detailed design is existing at present, but a remote steering launcher may be an attractive option.

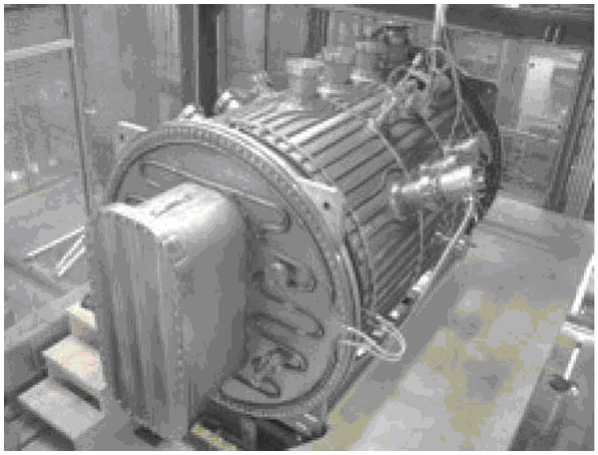

Fig. 20 Microwave stray radiation loading (MISTRAL) test facility.

3.2. In Vessel Structures

For the O2 and X3 ECH scenarios, where the incident beams will not be completely absorbed in the first path, microwave reflectors have to be installed at the inner vessel wall opposite to the steering mirrors. The beam will be reflected at an optimum angle to maintain a well-defined second path absorption in the plasma. Furthermore these reflectors prevent overheating of the vessel wall in CW-operation. The exact position was determined by ray-tracing calculations [4] as seen from Fig. 21, (left). These metallic tiles will be integrated in the graphite armour of the plasma-facing first wall and consist of a Titanium-Zirconium-Molybdenum (TZM) mirror surface, which is clamped on a water-cooled copper structure. An array of pick-up horns for the measurement of the transmitted beam profile and beam power incident on the mirror will be incorporated into each of the tiles. The thermal properties were simulated for different beam profiles. Assuming an incident microwave power of 0.5 MW, which corresponds to 50% single pass absorption, and a beam waste from ray tracing of 20 mm, the tile temperature reaches typically 300℃ (Fig. 21 (right)), which is acceptable. A test tile has been manufactured and is being prepared for high power test.

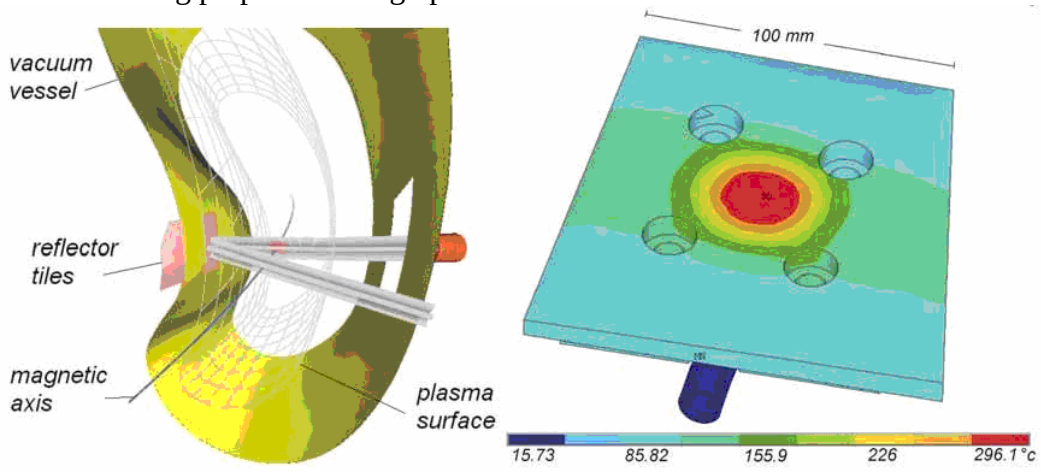

Fig. 21 Left: Ray-tracing calculation for the optimum position of the O2 and X3 reflector tiles at the in-board side of the W7-X plasma vessel. Right: Heat load simulation of a strongly focused ECH- beam (0.5 MW, beam waist 20 mm) at the TZM-reflector tile.

4. Summary and Conclusions

The ECH-system for the stellarator W7-X is the most ambitious and largest CW-plant presently under construction, its relevance for ITER is obvious.

The R&D phase for the gyrotrons and the transmission line was terminated and series production, installation and commissioning is in progress. The modular concept proved to be essential for the project realization, which runs on time and budget. MW-class 0.14 THz, CW-gyrotrons are now commercially available from two industrial manufacturers (TED and CPI). The successful full performance CW-tests (0.9 MW, 1800 s) of two single beam waveguide sections out of 10 ECH-modules have proven that the ECH-system is based on a viable and robust design. The quasi-optical multi-beam waveguide system offers favorable transmission characteristics close to the theoretical predictions and the most loaded components showed an excellent performance under full power, CW conditions.

The in-vessel components for W7-X are designed to provide CW-operation for all ECH scenarios. Intensive prototype tests have been performed in order to build a highly reliable system.

The test results and the operational experience may provide valuable input for the ITER-ECH system, because the physics demands and the main system parameters are comparable, while keeping in mind, that the ITER-system must satisfy additional requirements such as operation and maintenance in a radioactive environment.

Acknowledgments

The authors wish to thank the technical staff at FZK Karlsruhe, IPF Stuttgart and IPP Greifswald for their excellent contributions in solving numerous technological problems during the R&D of sophisticated ECH-components. We are grateful to the key persons at TED Velizy and CPI Palo Alto for their great effort and their readiness to incorporate innovative concepts in the gyrotron-R&D. Finally we would like to thank all partners in the collaborating European research laboratories for their stimulating discussions and active support.

This work was supported by the European Communities under the contract of Association between EURATOM and Forschungszentrum Karlsruhe, and was carried out within the framework of the European Fusion Development Agreement. The views and opinions expressed herein do not necessarily reflect those of the European Commission.

References

[1] V. Erckmann, H.J. Hartfuß, M. Kick, H. Renner, J. Sapper, F. Schauer, E. Speth, F. Wesner, F. Wagner, M. Wanner, A. Weller, H. Wobig: "The W7-X project: scientific basis and technical realization", *in Proc. 17th IEEE/NPSS Symposium on Fusion Engineering,* San Diego, USA (1997). Ed. IEEE, Piscataway, vol. 1, pp. 40-48 NJ (1998).

[2] M. Rome', V. Erckmann, U. Gasparino, N. Karulin: "Electron cyclotron resonance heating and current drive in the W7-X stellarator", *Plasma Phys. Control. Fusion*, vol. 40, pp. 511530(1998).

[3] H. P. Laqua, V. Erckmann, H.J. Hartfuß, H. Laqua, W7-AS Team, and ECRH Group: "Resonant and nonresonant

electron cyclotron heating at densities above the plasma cutoff by O-X-B mode conversion at the W7-AS stellarator", *Phys. Rev. Lett.*, vol. 78, pp. 34673470 (1997).

[4] V. Erckmann, P. Brand, H. Braune, G. Dammertz, G. Gantenbein, W. Kasparek, H.P. Laqua, H. Maassberg, N.B. Marushchenko, G. Michel, M. Thumm, Y. Turkin, M. Weissgerber, A. Weller, W7-X ECRH Team at IPP Greifswald, W7-X ECRH Team at FZK Karlsruhe and W7-X ECRH Team at IPF Stuttgart: "Electron cyclotron heating for W7-X: physics and technology", *Fusion Sci. Techno*l., vol. 52, pp. 291-312(2007).

[5] R. Heidinger, G. Dammertz, A. Maier, and M. Thumm: "CVD diamond windows studied with low and high power millimeter waves", *IEEE Trans. Plasma Sci.*, vol. 30, pp. 800807 (2002).

[6] G. Dammertz, S. Alberti, A. Arnold, E. Borie, V. Erckmann, G. Gantenbein, E. Giguet, R. Heidinger, J.P. Hogge, S. Illy, W. Kasparek, K. Koppenburg, M. Kuntze, H.P. Laqua, G. LeCloarec, Y. LeGoff, W. Leonhardt, C. Lievin, R. Magne, G. Michel, G. Müller, G. Neffe, B. Piosczyk, M. Schmid, M. Thumm, M.Q. Tran: "Development of a 140 GHz, 1 MW, continuous wave gyrotron for the W7-X stellarator", *IEEE Trans. Plasma Science*, vol. 30, pp. 808-818(2002).

[7] K. Felch, M. Blank, P. Borchard, P. Cahalan, S. Cauffman, T.S. Chu and H. Jory: "Recent advances in increasing output power andpulse duration in gyrotron oscillators", in *Conf. Digest 30th Int. Conf. on Infrared and Millimeter Waves and 13th Int. Conf. on Terahertz Electronics*, Williamsburg, VA, USA, pp. 237-238 (2005).

[8] K. Felch, M. Blank, P. Borchard, P. Cahalan, S. Cauffman, T.S. Chu and H. Jory: "Recent ITER-relevant gyrotron tests", *Journal of Physics: Conference Series*, vol. 25, pp. 13-23 (2005).

[9] H. Jory, M. Blank, P. Borchard, P. Calahan, S. Cauffman, T.S. Chu, K. Felch: "CPI gyrotrons for fusion EC heating", in *Proc. 7th Workshop on High Energy Density and High Power RF, AIP Conference Proceedings 807*, pp. 180-190 (2006).

[10] M. Thumm, X. Yang, A. Arnold, G. Dammertz, G. Michel, J. Pretterebner, D. Wagner: "A high-efficiency quasi-optical mode converter for a 140-GHz 1-MW CW gyrotron", *IEEE Trans. on Electron Devices*, vol. 52, pp. 818-824 (2005).

[11] G. Dammertz, S. Alberti, A. Arnold, D. Bariou, P. Brand, H. Braune, V. Erckmann, G. Gantenbein, E. Giguet, R. Heidinger, J.P. Hogge, S. Illy, J. Jin, W. Kasparek, K. Koppenburg, H.P. Laqua, F. Legrand, W. Leonhardt, C. Liévin, R. Magne, G. Michel, G. Müller, G. Neffe, B. Piosczyk, T, Rzesnicki, M. Schmid, M. Thumm, M. Q. Tran and X. Yang: "Development of multimegawatt gyrotrons for fusion plasma heating and current drive", *IEEE Trans. on Electron Devices*, vol. 52, pp. 808-817 (2005).

[12] G. Dammertz, S. Alberti, A. Arnold, D. Bariou, P. Brand, H. Braune, V. Erckmann, O. Dumbrajs, G. Gantenbein, E. Giguet, R. Heidinger, J.P. Hogge, S. Illy, J. Jin, W. Kasparek, K. Koppenburg, H.P. Laqua, F. Legrand, W. Leonhardt, Ch. Liévin, G. Michel, G. Müller, G. Neffe, B. Piosczyk, O. Prinz, T. Rzesnicki, M. Schmid, M. Thumm, M.Q. Tran, X. Yang, and I. Yovchev: "High-power gyrotron development at Forschungszentrum Karlsruhe for fusion applications", *IEEE Trans. Plasma. Sci.*, vol. 34, pp. 173-186 (2006).

[13] M. Thumm, S. Alberti, A. Arnold, P. Brand, H. Braune, G. Dammertz, V. Erckmann, G. Gantenbein, E. Giguet, R. Heidinger, J.P. Hogge, S. Illy, W. Kasparek, H.P. Laqua, F. Legrand, W. Leonhardt, C. Liévin, G. Michel, G. Neffe, B. Piosczyk, M. Schmid, K. Schwörer, M.Q. Tran: "EU megawatt-class 140-GHz CW gyrotron", *IEEE Trans. on Plasma Sci.*, vol. 35, pp. 143-153(2007).

[14] G. Dammertz, S. Alberti, D. Fasel, E. Giguet, K. Koppenburg, M. Kuntze, F. Legrand, W. Leonhardt, C. Lievin, G. Müller, G. Neffe, B. Piosczyk, M. Schmid, A. Sterk, M. Thumm, M.Q. Tran, A.G.A. Verhoeven: "Power modulation capabilities of the 140 GHz/1MW gyrotron for the stellarator Wendelstein 7-X", *Fusion Eng. Des.*, vol. 66-68, pp. 497-502 (2003).

[15] M. Schmid, S. Illy, G. Dammertz, V. Erckmann, M. Thumm: "Transverse field collector sweep system for high power

CW gyrotrons", *Fusion Eng. Des*., vol. 82, pp. 744-750(2007).

[16] V. Erckmann, W7-X ECRH teams at IPP, IPF and FZK: The W7-X "ECRH plant: status and recent achievements", in *Proc. 17th Topical Conf. on Radio Frequency Power in Plasmas*, Clearwater, Florida, USA, AIP Conf. Proc. vol. 933, pp. 421-424 (2007).

[17] M. Thumm and W. Kasparek: "Passive high-power microwave components", *IEEE Trans. on Plasma Sci*., vol. 30, pp. 755-786(2002).

[18] W. Kasparek, H. Kumric, G.A. Müller, P.G. Schüller, V. Erckmann: High power microwave generation and applications, D. Akulina, E Sidoni and C. Wharton, eds., *Societa Italiana di Fisica*, ISBN 88-7794-044-1, Bologna (1992).

[19] L. Empacher, W. Förster, G. Gantenbein, W. Kasparek, G.A. Müller, P.G. Schüller, K. Schwörer, U. Schumacher, D. Wagner, V. Erckmann, T. Geist, H. Laqua: "Conceptual design of the 140 GHz/10 MW CW ECRH system for the stellarator W7-X", *Fusion Technology 1*996, Amsterdam: Elsevier Science B.V., pp. 541-544 (1997).

[20] W. Grau, in W. Kleen, and R. Müller: *Laser.* Berlin: Springer (1969).

[21] P.F. Goldsmith: Quasi-optical Systems. *New York: IEEE Press*, Chapman and Hall, Publishers, ISBN 0-7803-3439-6 (1998).

[22] J.A. Murphy: "Distortion of a simple Gaussian beam on reflection from off-axis ellipsoidal mirrors", *Int. J. Infrared Millim. Waves*, vol. 8, pp. 1165 – 1187 (1987).

[23] D. Vinogradov: "Mirror conversion of gaussian beams with simple astigmatism", *Int. J. Infrared Millim. Waves*, vol. 16, pp. 1945-1963 (1995).

[24] L. Empacher and W. Kasparek: "Analysis of a multiple-beam waveguide for free-space transmission of microwaves", *IEEE Trans. Antennas Propagat*., vol. 49, pp. 483-493(2001).

[25] K.W. Kopp, W. Kasparek, E. Holzhauer: "Microwave reflection properties of grooved metallic mirrors", *Int. J. Infrared Millim*. Waves, vol. 13, pp. 1919-1631 (1992).

[26] L. Empacher, W. Förster, G. Gantenbein, W. Kasparek, H. Kumric, G.A. Müller, P.G. Schüller, K. Schwörer, D. Wagner, H. Brinkschulte, V. Erckmann, T. Geist, H. Laqua, F. Leuterer, G. Münich: "New developments and tests of high power transmission components for ECRH on ASDEX-Upgrade and W7-AS", in *Proc. 20th Int. Conf. on Infrared and Millimeter Waves*, Lake Buena Vista, pp. 473-474 (1995).

[27] R. Winston, "Light collection within the framework of geometric optics", *J. Opt. Soc*. Amer., vol. 60, pp. 245-247 (1970).

[28] W. Kasparek, A. Fernandez, F. Hollmann, and R. Wacker: "Measurements of Ohmic losses of metallic reflectors at 140 GHz using a 3-mirror resonator technique", *Int. J. Infrared and Millim. Waves*, vol. 22, pp. 1695-1707 (2001).

[29] H. Hailer, G. Dammertz, V. Erckmann, G. Gantenbein, F. Hollmann, W. Kasparek, W. Leonhardt, M. Schmid, P.G. Schüller, M. Thumm, M. Weissgerber: "Mirror development for the 140 GHz ECRH system of the stellarator W7-X", *Fusion Eng. Des.*, vol. 66-68, pp, 639–644 (2003).

[30] W. Kasparek, P. Brand, H. Braune, G. Dammertz, V. Erckmann, G. Gantenbein, F. Hollmann, M. Grünert, H. Kumric, L. Jonitz, H.P. Laqua, W. Leonhardt, G. Michel, F. Noke, B. Plaum, F. Purps, M. Schmid, T. Schulz, K. Schwörer, M. Thumm, M. Weissgerber: "Status of the 140 GHz, 10 MW CW transmission system for ECRH on the stellarator W7-X",

Fusion Eng. Des., vol. 74, pp. 243-248(2005).

[31] L. Empacher, W. Förster, G. Gantenbein, W. Kasparek, H. Kumric, G.A. Müller, P.G. Schüller, K. Schwörer, U. Schumacher, D. Wagner, H. Zohm and V. Erckmann: "Calculations and experiments on multi-beam transmission for the 140 GHz/10 MW CW ECRH system on W7-X", in Proceedings of the 10th Joint Workshop on ECE and ECRH, ed. T. Donne and A.G.A. Verhoeven, *Singapore: World Scientific*, pp. 561-568 (1997).

[32] J. Shi and W. Kasparek: "A grating coupler for in-situ alignment of a Gaussian beam – principle, design, and low-power test", *IEEE Trans. Antennas Propagat*., vol. AP-5, pp. 2517 – 2524(2004).